Original Article

Cardiac Contraction Motion Correction in Gated Myocardial Perfusion SPECT Projection Domain

Narges Salehi[1, 2], Emad Fatemizadeh[3], Mohammad Hossein Farahani[2], Afshin Akbarzadeh[2], Saeed Farzanefar[4], Mohammad Reza Ay [1, 2,*]

1- Department of Medical Physics and Biomedical Engineering, School of Medicine, Tehran University of Medical Science, Tehran, Iran.

2- Research Center for Molecular and Cellular Imaging, Tehran University of Medical Sciences, Tehran, Iran.

3- Electrical Engineering Department, Sharif University of Technology, Tehran, Iran.

4- Department of Nuclear Medicine, Vali-Asr Hospital, School of Medicine, Tehran University of Medical Sciences, Tehran, Iran.

Received: 18 September 2015
Accepted: 5 November 2015

ABSTRACT

Purpose- Cardiac contractions and respiratory movements are two main factors which degrade gated myocardial perfusion SPECT images quality by inducing image blurring and also causing quantification inaccuracies. We propose a non-rigid motion correction step before the image summation in order to eliminate the influence of cardiac motion on MPS images. Motion correction in image domain using intensity based image registration algorithm is quite time consuming. Therefore, in order to reduce the computation time, we introduced a method which works on projection domains and is fast compared to image domain correction methods.

Material and Method- We studied the effect of our motion correction method on the projection data using simulation as well as patient data. The mathematical four-dimensional NURBS-based Cardiac-Torso phantom with two different heart sizes (124 ml and 100 ml left ventricular cavities) were constructed for male and female, respectively. SIMIND Monte Carlo simulation package was used to simulate a clinical Tc99-mibi perfusion SPECT acquisition protocol on the dual headed gamma camera (Philips Medical Systems, Cleveland, Ohio), with Low Energy High Resolution (LEHR) collimators. We have warped each frame, with respect to end diastolic frame, using a 3D dimensional non-parametric diffeomorphic algorithm based on Thirion Demon registration technique in MATLAB 2015. 4D sequence of motion corrected projections and the original projection data were reconstructed using FBP algorithm in AutoRecon application in Cedars Sinai package. Myocardial thickness, myocardium to blood pool contrast and CNR were measured in summed images before the correction and motion corrected (BC and MC respectively). Quantitative study of image sequences were conducted after importing image sequences to cardiac SPECT system's work station. Total perfusion defect (TPD) scores of each of BC and MC summed images were automatically derived and calculated using standard Cedars-Sinai software. Gated images were motion compensated using Motion Freezing (MF) application on Cedars-Sinai software and TPD of Motion Frozen (MF) data were also generated so as to compare our methods quantification results with an image based motion correction method.

Result- Myocardial wall thickness in the lateral wall is reduced to 11% from BC images to MC images in patient study which is statistically significant. Myocardium to blood pool contrast in MC images are greater than the corresponding summed images before the correction (BC) (27.10±11.07 vs. 32.55±12.07 (P=0.006)), CNR has increased 31% (P=0.02) in MC images compared to corresponding BC images.

***Corresponding Author**
Mohammad Reza Ay, PhD
Department of Medical Physics and Biomedical engineering, School of Medicine, Tehran University of Medical Science, Tehran, Iran.
Tel/Fax: (+98) 2166907518
E-mail: mohammadreza_ay@tums.ac.ir

Keywords:
Myocardial perfusion SPECT,
Cardiac contraction,
Motion correction,
Projection domain,
Diffeomorphic demons.

Total Perfusion Defect (TPD) measure before and after the correction were highly correlated. TPD of MC and MF images had no statistically significant difference.

Conclusion- Motion correction in projection domain may increase the image quality by reducing the blurring due to cardiac motion and possibly intra frame motion. Higher myocardial to blood pool contrast and CNR were obtained in this study. It is highly recommended that with the correction we can improve defect detectability and diagnostic value of images, further assessment with a large patient population is under evaluation.

1. Introduction

Myocardial perfusion can be assessed using a single photon emission computed tomography (SPECT) [1]. Cardiac and respiratory motion cause severe artifacts and spatial blurring in myocardial perfusion SPECT images [2].

Respiratory motion is more or less locally rigid while cardiac motion is highly non-linear [3]. Endocardial motion range between end-diastolic (ED) and end-systolic (ES) frames has been reported 13±2 mm,14±2 mm for male and female respectively and 12±2 mm for both genders in epicardial displacement [4]. Currently, several clinical protocols such as static and gated acquisitions are available. The noise problem is even more severe in cardiac-gated SPECT which is proposed to solve motion problem by separating photon counts into cardiac phases. Gating reduces the contraction motion impact in each time frame but at the cost of elevating the noise level due to low count density at each gate [5]. Motion correction in gated myocardial perfusion SPECT (MPS) mainly is based on non-rigid summation of gated frames. Many methods have been suggested for the cardiac motion correction in image domain. Klein *et al*. proposed a method for summing PET gated data. This technique finds a mapping between each voxel of two gated volume, based on the optical flow technique by modeling non-rigid motion of the heart during cardiac cycle [6]. Maire *et al*. investigated a simultaneous estimation of non-rigid motion vector field and image reconstruction. They presented a pixel based method by defining an objective function consisting of ML-image reconstruction term, elastic material's strain energy and image matching term [7]. Slomka *et al*. proposed a motion estimation technique by tracking endocardial and epicardial surfaces which compensated for the motion to these surfaces, clinically known as "Motion Frozen" [4]. Suzuki *et al*. studied a diagnostic performance of the standard SPECT and motion-frozen (MF) myocardial perfusion SPECT (MPS) in obese patients and their results demonstrated an improvement in CAD detection in obese patients [8]. Kovalski *et al*. introduced "dual motion frozen heart" combining respiration and contraction compensation in gated myocardial perfusion SPECT. Compensating for both respiration and cardiac contraction and contraction correction had a great effect on perfusion images resulting in significantly improved image quality [9]. Marin *et al*. defined a temporal smoothing constraint during maximum likelihood reconstruction by tracking myocardial motion using a deformable mesh model for the motion compensated reconstruction of gated cardiac SPECT images [10]. Some of these proposed methods are performed on image domain and some are applied during image reconstruction. The general scheme of cardiac motion correction on image domain is to transform reconstructed cardiac frames into a reference frame in order to reduce motion-blurring effects. The resulted static image obtained by summing up different frames has significantly lower image noise without resolution degradation [11]. Feng *et al*. [12] studied motion correction before (MCBR), after (MCAR) and during (MCDR) image reconstruction and they have shown that the motion correction in MCDR is more accurate and allows a better quantification in high count images. MCBR's great advantage was the dramatic reduction of computation time and an accurate quantification for low count images.

In this study, we introduce a method to amend the effect of cardiac contraction motion in projection domain of myocardial perfusion SPECT studies using a totally unconstrained diffeomorphic registration method which is well suited for non-linear deformations.

2. Materials and Methods

2.1. Simulation Study

4D NURBS-based cardiac-torso phantom (NCAT) [13] with realistic models of anatomy, respiratory and cardiac motions, with an activity and photon attenuation among the tissues organs was employed to simulate a clinical Tc-99m cardiac gated SPECT perfusion study [14, 15].

The SIMIND Monte Carlo simulation tool was used to simulate data acquisition, including degradations due camera response, scatter and non-uniform attenuation. The simulated field of view (FOV) was 40 cm with voxel size of 0.64 cm. The uncorrected intrinsic system FWHM at the center of the FOV was approximately 0.34 cm. Poisson noise was introduced at a level corresponding to 0.5×10^6 counts originating from the heart region and a total of 8 frames were simulated. Each frame had 32 projections over 180° and 64 × 64 projection bins. This corresponds to the dual headed Philips (ADAC-forte) gamma camera (Philips Medical Systems, Cleveland, Ohio), with Low Energy High Resolution (LEHR) collimators.

2.2. Clinical Acquisition Protocol

2.2.1. Patient Population

We used available data retrospectively from the nuclear cardiology database at department of Nuclear Medicine, Vali-Asr Hospital, School of Medicine, Tehran University of Medical Sciences, Tehran, Iran. We studied 18 patients including 13 female and 5 male (48-87 years; BMI of 30.1–46.8) without knowing about their cardiac condition. They underwent both standard supine rest /stress 99m-Tc gated MPS. Prior to data acquisition patients underwent either exercise or adenosine stress protocols as described in refrence. [16].

2.2.2. Acquisition and Reconstruction Protocols

MPS acquisitions were obtained using noncircular orbits and 32 projections over 180 degrees (45 right anterior oblique to 45 left posterior oblique) at 25 second/projection for Tc-99m -sestamibi. MPS. All images were subject to standard clinical quality-control measures [16].

2.3. Spatial Transformation

In this study, we assumed that existing motions in the projection space are exactly mapped to the image space. Myocardial motion estimation along sequences is regarded as a succession of projection-set to projection-set registration problems. Correction displacement fields from the initial frame which is End-Diastolic (ED) frame to all following frames is required for cardiac motion [17]. We used a symmetric diffeomorphic demon algorithm which is a totally unconstrained registration method on diffeomorphism space in order to find displacement fields between frames. This method is based on the optical flow constraint and requires neither a segmentation nor a matching step. The main requirement of this method is that the intensities in both images must be comparable which is realized in our case since projection frames are acquired through a single study and there is a temporal coherence between the sequence [18]. The key idea of this method is to find an optimal non-rigid and symmetric velocity vector field by computing the corresponding update field via minimizing an energy functional (equation 1) defined on points of projections attained from myocardium [19].

$$E(c,s) = \left\| \frac{1}{\sigma_i}(F - M \circ c) \right\|^2 + \frac{1}{\sigma_x} dist(s,c)^2 + \frac{1}{\sigma_T} Reg(s) \quad (1)$$

Where F is template projections which in our case would be ED frame and M is moving projections, spatial transformation are defined as, s which is the displacement field. In order to symmetrize this algorithm, we computed a demon in two steps for forward forces and backward forces and a Gaussian kernel with K_{fluid} was convolved for fluid like regularization in order to update the vector field. A Gaussian kernel with K_{diff} was convolved for diffusion like regularization in order to deform the vector field [20]. Topology preserving/homeomorphic algorithms like diffeomorphic demons produce a mapping that is continuous onto and locally one to one and also has a continuous inverse. The Jacobian determinant contains information regarding the injectivity of the mapping and is greater than zero for topology preserving mappings [21]. Therefore, in order to evaluate the physical plausibility of deformation, we examined the singularities. A deformation must be

one to one so that regions, where the deformation field is not bijective, are referred as singularities. We subsequently calculated the determinant of the Jacobian of the deformation field at every point [22]. Each point with Jacobian ≤ 0 denotes a singularity [23].

2.4. Image Reconstruction

All projection in both data sets were reconstructed by filtered back projection (FBP) algorithm with Butterworth (cutoff=0.4 Hz, order=10) and then short-axis slices were automatically generated using AutoRecon application on Cedars-Sinai package (version 2013.1) [24]. No attenuation and scatter correction was used.

2.5. Registration Effects Validation

In order to validate our registration method's effect on the projection data, we have designed an XCAT phantom which has a defect in the inferior wall. We, then, simulated the SPECT study with SIMIND Monte Carlo package and reconstructed them using FBP (cutoff=0.4 cycles/cm, order=10). We considered the total perfusion defect (TPD) of both images as a criterion of the number of hyper-perfused pixels. The TPD of the reconstructed summed image has been chosen as the gold standard.

2.6. Image Parameters

Volume of interest over the LV and blood pool were generated via AMIDE software. Mean and standard deviation (SD) values were calculated for each data set for both myocardium and blood pool. We subsequently calculated the following metrics:

2.6.1. Myocardium to Blood Contrast and CNR

Contrast and CNR were calculated globally for static summed images and motion corrected images [25].

$$Myocardium\ to\ blood\ contrast = \frac{\mu_{LV} - \mu_{blood}}{\mu_{LV} + \mu_{blood}} \quad (2)$$

$$CNR = \frac{\mu_{LV} - \mu_{blood}}{\sigma_{blood}} \quad (3)$$

Where μ_{LV}, μ_{blood} and are the mean number of counts of the myocardium and blood pool and standard deviation of count in blood pool, respectively.

2.6.2. Myocardial Wall Thickness

Line profiles were taken across the lateral wall of the left ventricle which has the largest motion [26, 27]. The distance between the ascending and descending flanks of the profile curve was taken as the width of the myocardial wall. The line profile was fitted with a Gaussian curve and the FWHM of the fitting function was used. Three consecutive middle slices were selected to reduce the noise influence and the average wall thickness was calculated [26].

2.6.3. TPD

Total Perfusion Deficit (TPD) of summed images before and after the motion correction (TPD-BC and TPD-MC, respectively) were automatically derived and calculated on the basis of sex specific normal limits obtained from a healthy population using standard Cedars-Sinai software [28].

2.6.4. Motion Freezing (MF)

This image-processing technique is an application on Cedars-Sinai software and compensates for the cardiac contraction motion by tracking endo- and epicardial borders of Left Ventricle (LV) and it also generates displacement vectors between end-diastole and other gated frames [4].

2.7. Statistical Analysis

All statistical analysis were performed using SPSS Statistics Version 21. All continuous variables are expressed as mean ±SD. Paired-T tests were used to compare differences in paired continuous normally distributed data. Wilcoxon rank sum test was used for non-normally distributed data. All statistical tests were 2-tailed, and a P value of less than 0.05 was considered significant.

3. Results

The aforementioned algorithm was implemented on 7 cardiac gated projection data with respect to End-Diastolic (ED) projections.

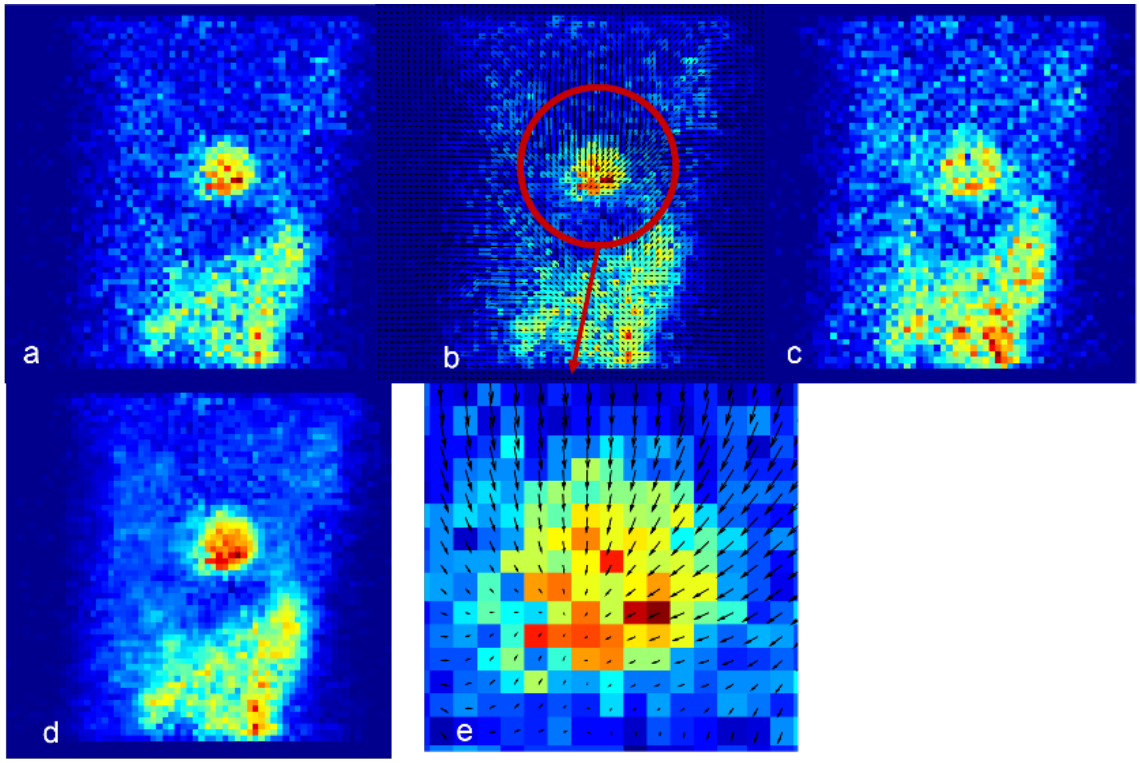

Figure 1. Implementing the diffeomorphic demon algorithm on projection data. a) End-Systolic frame projections middle slice b) ES frame with corresponding displacement vectors from ES to ED overlaid c) ED frame projections middle slice d) Warped ES frame.

3.1. Registration Validation

The TPD of the reconstructed summed image has been chosen as the gold standard. It was 54% and the TPD the of the motion corrected reconstructed images was 52% as long as the TPD shows the extent of defect in pixel level, it is concluded that the number of under-perfused pixels in the corrected image has not been significantly different from summed standard image.

3.2. Simulation Study

3.2.1. Wall Thickness

The measured thickness in female phantom was 13.33 mm before the correction and after the correction, it was reduced to 11.24 mm. The male phantom thickness was measured 7.40 and 7.05 before and after the correction respectively.

3.2.2. Contrast and CNR

Myocardium to blood pool contrast and CNR has increased to 69% and 95% respectively for male phantom and 35% and 0.89% respectively for the female phantom.

3.3. Patient Study

3.3.1. Wall Thickness

The measured thickness in data sets were significantly different; the thickness of the summed image for 18 patients was 9.74±1.79 mm and 8.60±1.11 mm before and after the correction respectively (P=0.004).

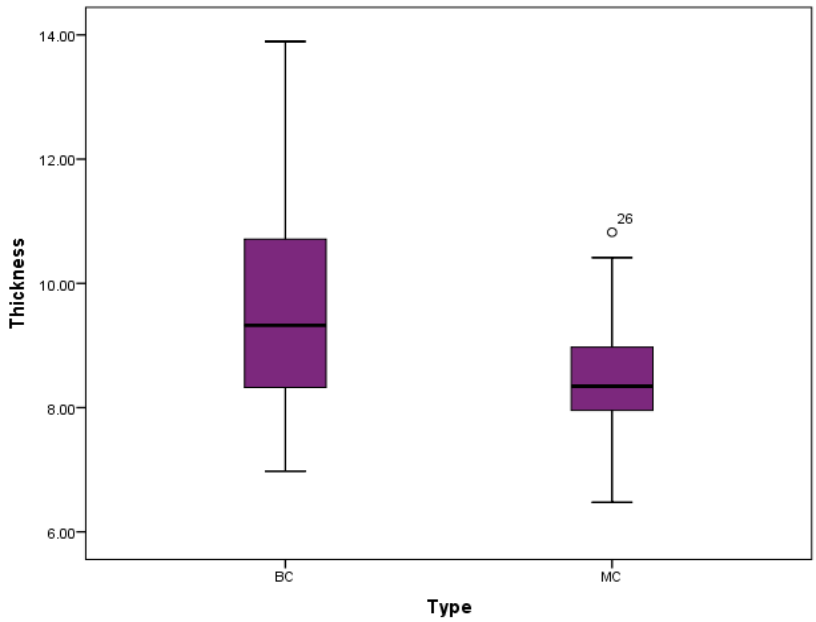

Figure 2. Lateral wall thickness (mm) before (BC) and after correction (MC).

3.3.2. Contrast and CNR

The myocardium-to-blood contrast changed significantly between the uncorrected and corrected images as shown in Figure 3. Figure 4 provides CNR results on a per-patient basis. Examples of improvements in terms of the visual image quality before and after the motion correction in projection space can be seen in Figures 5 and 6.

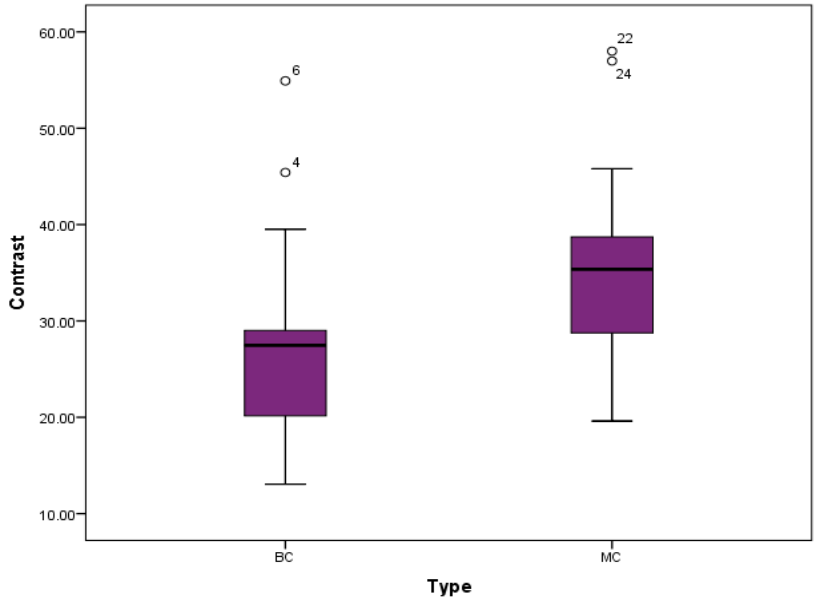

Figure 3. Myocardial to blood contrast for cardiac images before (BC) and after (MC) the motion correction.

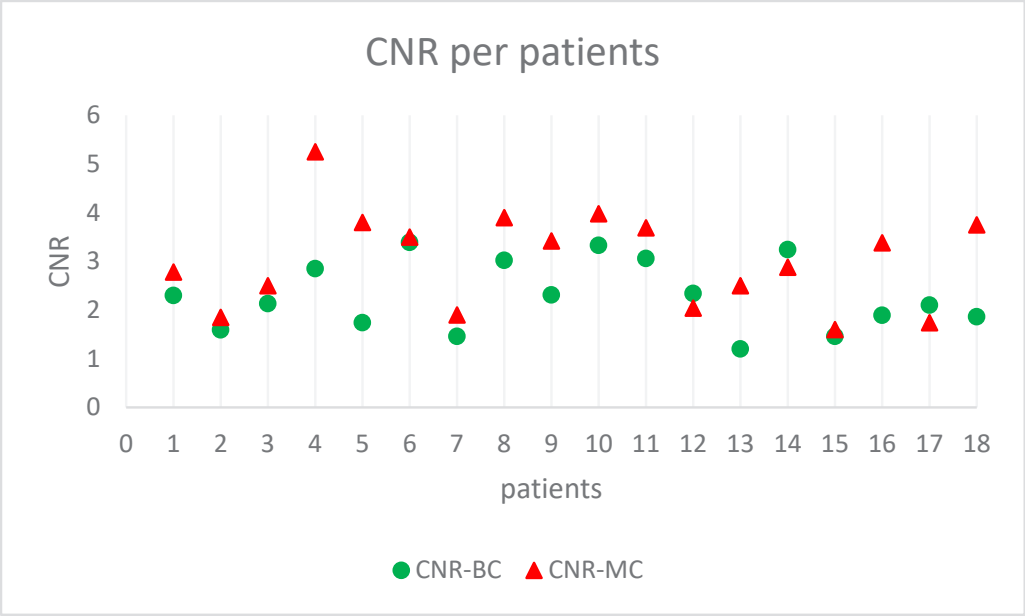

Figure 4. CNR for images before (BC) and after (MC) the correction for each 18 patients.

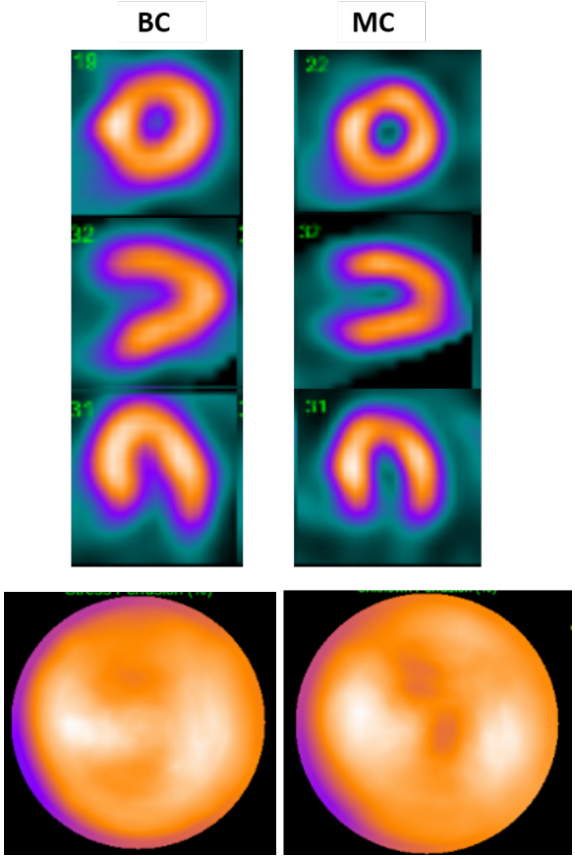

Figure 5. A 61-y female patient with low likelihood of CAD, weight=78 kg underwent gated stress imaging with Tc-99 mibi, BC= Before the motion correction and AC= After the motion correction.

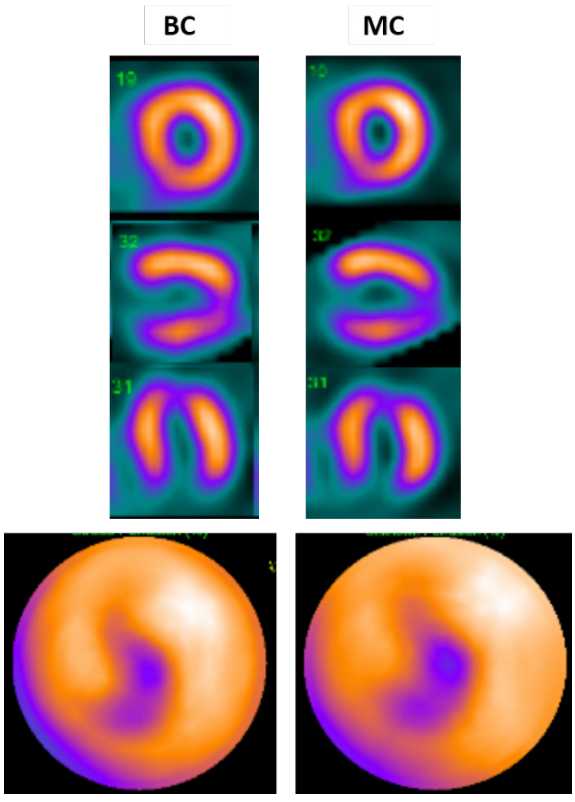

Figure 6. A 58-y male patient with no prior knowledge, weight=83 kg underwent gated stress imaging with Tc-99 mibi, BC= Before the motion correction and AC= After the motion correction.

3.3.3. TPD

A Pearson product-moment correlation coefficient was computed to assess the relationship between the TPD-BC and TPD-MC. There was a positive correlation between the two variables [r =0.90, n =18, P<0.0001]. A scatterplot summarizes the results (Figure 7).

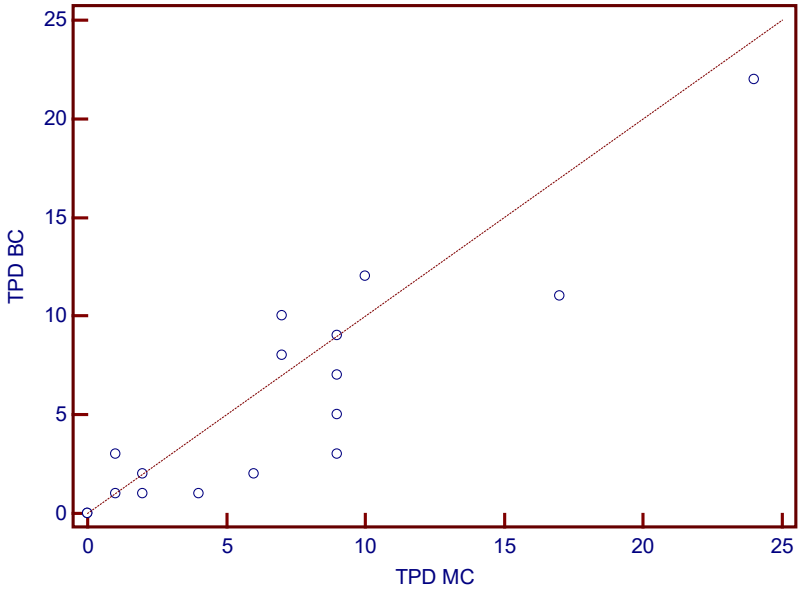

Figure 7. Comparison of TPD measure before (BC) and after the motion correction (MC).

TPD results of Motion Frozen (MF) images were also compared to MC images and there were no statistically significant difference between MC and MF TPDs (P-Value=0.07). There was a positive correlation between the two variables [r =0.87, n =18, P<0.0001].

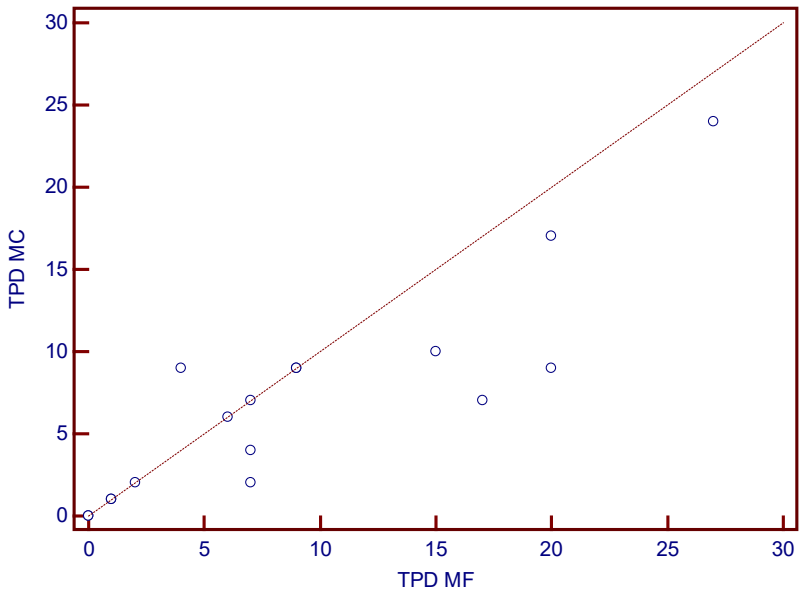

Figure 8. Comparison of TPD measure of Motion Frozen (MF) and after the motion correction with proposed algorithm (MC).

4. Discussion

The goal of the motion correction method is to compensate for myocardial motion in the different phases of the ECG-gated SPECT data. We intended to establish a cardiac motion-compensated pre-reconstruction processing method that can be applied regardless of the image reconstruction methods used. In this paper, we have shown that the cardiac motion and possibly intra-frame motion correction in the projection domain is possible. In the current study, we assumed that the motion in the projection domain is similar to the motion existing in the image domain. Therefore, motion transformation in the projection domain is related to the transformation matrix in the image domain [12]. The advantage of performing the motion correction before the image reconstruction is not only much faster compared with post processing approaches, it is also possible to correct for an intra-frame motion and even allows event by event correction using list mode data [11].

In order to yield excellent temporal summation results, we must characterize the motion accurately. So the most critical step in the motion correction pre-processing is the estimation of cardiac motion. We used a symmetric diffeomorphic demon algorithm which is a totally unconstrained nonparametric and a non-rigid registration method and robust to noise. Therefore, it is totally unrestricted regarding the allowed deformations. As long as demons produced smooth deformation and the voxels presented no singularity, this suggests that diffeomorphic demons produce realistic deformations and the motion is physiologically acceptable [23]. The accuracy of deformable registration is a very important step, registration validation remains a challenging problem in practice mainly due to the lack of 'ground truth' [29]. Since there were no validation techniques available for using diffeomorphic algorithms in the projection domain, we tried to validate our method on the image domain using gold standard phantom images. As the validation results has shown, there were no difference between hyper-perfused pixels in the standard image and corrected image. A validation

technique for the motion correction in the projection domain will be investigated in our future work.

As it is shown in Figure 2, the measured myocardial lateral wall thickness after motion correction between male and female phantom has a large difference. Since the male phantom has a large heart, the limited resolution of the system does not cause too much spill over following thickening of the wall. However, the female phantom has a very small heart and lost its resolution due to PVE in systolic frames and the resultant summed image suffers from thickening and the loss of contrast. As long as our motion correction algorithm is not mass-preserving and does not take PVE into account [3], it cannot have a significant effect in such cases. However, it still works better than the MF since it is a landmark based registration and when endocardial points are not distinguishable in systolic frames, a motion compensation would be impossible [4]. The wall thickness in patients has been decreased to 11% which was statistically significant and is due to a motion induced blurring reduction in the lateral wall which has the largest motion.

Myocardial to blood pool contrast have increased significantly compared to corresponding uncorrected summed images (27.10±11.07 vs. 32.55±12.07) (Figure 2). In the end-systolic phase the blood pool is small and LV walls are closer to each other due to the muscle contraction and therefore are thicker. Accordingly, there is a greater blurring effect compared to the end-diastolic phase when the blood pool is larger and the walls are farther apart [30]. After summation of all frames, systolic frames reduce the myocardium to blood pool contrast and cause a quality degradation and quantification inaccuracy [27]. As it is shown in Figure 5 and 6, myocardium to blood pool contrast in motion corrected images is visually better than corresponding uncorrected images. Besides, the apparent CNR has increased in corrected images (31%) which indicates an image quality improvement after the motion correction as long as the blurring due to the motion is decreased when the image SNR is intact.

TPD results presented in Figure 7 and Figure 8 show that our approach is equivalent to both standard quantitative method and an image based motion compensation method.

Nonetheless, the apparent myocardium/blood pool contrast and CNR have increased; the clinical significance of these improvements in the perfusion abnormality detection and diagnostic value of this method will need to be investigated due to the small sample size (n=18).

Myocardial motion generated by respiration and cardiac contraction during MPI-SPECT affects the image quality and may introduce image artifacts. Motion correction in the projection domain may increase the image quality by reducing the blurring due to the cardiac motion and possibly intra frame motion. Myocardium to blood pool contrast and CNR has increased to 19% and 31% respectively, which indicates a higher image quality after the motion correction. It is highly recommended that the defect detectability and diagnostic value of images can be improved with the correction. Further studies are highly recommended.

Acknowledgements

This work was supported by the Tehran University of Medical Sciences, Tehran, Iran under grant number 27463.

References

1- C. L. Hansen, R. A. Goldstein, O. O. Akinboboye, D. S. Berman, E. H. Botvinick, K. B. Churchwell, *et al.*, "Myocardial perfusion and function: single photon emission computed tomography," *J Nucl Cardiol,* vol. 14, pp. e39-60, Nov-Dec 2007.

2- M. Dawood, F. Buther, X. Jiang, and K. P. Schafers, "Respiratory motion correction in 3-D PET data with advanced optical flow algorithms," *IEEE Trans Med Imaging,* vol. 27, pp. 1164-75, Aug 2008.

3- F. Gigengack, L. Ruthotto, M. Burger, C. H. Wolters, X. Jiang, K. Sch, *et al.*, "Motion correction of cardiac PET using mass-preserving registration," in *IEEE Nuclear Science Symposuim & Medical Imaging Conference*, pp. 3317-9, 2010.

4- P. J. Slomka, H. Nishina, D. S. Berman, X. Kang, C. Akincioglu, J. D. Friedman, *et al.*, ""Motion-frozen" display and quantification of myocardial perfusion,"

Journal of Nuclear Medicine, vol. 45, pp. 1128-1134, 2004.

5- G. L. Zeng, G. T. Gullberg, and E. Debreuve, "Projection data registration for gated cardiac SPECT reconstruction," in *Nuclear Science Symposium Conference Record, 2002 IEEE*, pp. 1516-8, 2002.

6- G. Klein, B. Reutter, and R. Huesman, "Non-rigid summing of gated PET via optical flow," *Nuclear Science, IEEE Transactions on,* vol. 44, pp. 1509-1512, 1997.

7- B. A. Mair, D. R. Gilland, and Z. Cao, "Simultaneous motion estimation and image reconstruction from gated data," in *Biomedical Imaging, 2002. Proceedings. 2002 IEEE International Symposium on*,pp. 661-4, 2002.

8- Y. Suzuki, P. J. Slomka, A. Wolak, M. Ohba, S. Suzuki, L. De Yang*, et al.*, "Motion-frozen myocardial perfusion SPECT improves detection of coronary artery disease in obese patients," *J Nucl Med,* vol. 49, pp. 1075-9, Jul 2008.

9- G. Kovalski, Z. Keidar, A. Frenkel, J. Sachs, S. Attia, and H. Azhari, "Dual "motion-frozen heart" combining respiration and contraction compensation in clinical myocardial perfusion SPECT imaging," *J Nucl Cardiol,* vol. 16, pp. 396-404, May-Jun 2009.

10-T. Marin, M. N. Wernick, Y. Yang, and J. G. Brankov, "Motion-compensated reconstruction of gated cardiac SPECT images using a deformable mesh model," in *2010 IEEE International Symposium on Biomedical Imaging: From Nano to Macro*, pp. 520-3, 2010.

11- T. Feng, J. Wang, G. Fung, and B. Tsui, "Non-rigid dual respiratory and cardiac motion correction methods after, during, and before image reconstruction for 4D cardiac PET," *Phys Med Biol,* vol. 61, pp. 151-68, Jan 7 2016.

12- T. Feng and B. M. Tsui, "Non-rigid respiratory motion correction for 4D gated PET sinogram data," in *Nuclear Science Symposium and Medical Imaging Conference (NSS/MIC), 2013 IEEE*, pp. 1-5, 2013.

13- W. Segars, G. Sturgeon, S. Mendonca, J. Grimes, and B. M. Tsui, "4D XCAT phantom for multimodality imaging research," *Medical physics,* vol. 37, pp. 4902-4915, 2010.

14- W. P. Segars, B. Tsui, D. Lalush, E. Frey, M. King, and D. Manocha, "Development and application of the new dynamic Nurbs-based Cardiac-Torso (NCAT) phantom," 2001.

15- A. K.-A. Zohreh Shahpouri, Ahmad Bitarafan-Rajabi, Jakir Hossain, Seyed Mohammad Entezarmahdi, Samane Mohseni, Nahid Yaghoob, Arman Rahmim, "A Comparative Assessment of Dynamic and Conventional Thallium-201 SPECT Myocardial Perfusion Imaging: Monte Carlo Simulations and Case Studies " *frontiers in biomedical technology,* vol. 1, pp. 91-102, 2014.

16- T. Holly, B. Abbott, M. Al-Mallah, D. Calnon, M. Cohen, and F. DiFilippo, "ASNC imaging guidelines for nuclear cardiology procedures. Single photon-emission computed tomography. 2010," ed, 2011.

17- O. Somphone, M. De Craene, R. Ardon, B. Mory, P. Allain, H. Gao*, et al.*, "Fast myocardial motion and strain estimation in 3D cardiac ultrasound with sparse demons," in *Biomedical Imaging (ISBI), 2013 IEEE 10th International Symposium on*, pp. 1182-5, 2013.

18- E. Debreuve, M. Barlaud, I. Laurette, G. Aubert, and J. Darcourt, "Nonparametric and nonrigid registration method applied to myocardial-gated SPECT," *IEEE Transactions on Nuclear Science,* vol. 49, pp. 782-788, 2002.

19- T. Vercauteren, X. Pennec, A. Perchant, and N. Ayache, "Diffeomorphic demons: Efficient non-parametric image registration," *NeuroImage,* vol. 45, pp. S61-S72, 2009.

20- T. Vercauteren, X. Pennec, A. Perchant, and N. Ayache, "Symmetric log-domain diffeomorphic registration: A demons-based approach," in *Medical Image Computing and Computer-Assisted Intervention–MICCAI 2008*, ed: Springer, 2008, pp. 754-761.

21- A. Sotiras, C. Davatzikos, and N. Paragios, "Deformable Medical Image Registration: A Survey," *IEEE transactions on medical imaging,* vol. 32, pp. 1153-1190, 2013.

22- D. Rey, G. Subsol, H. Delingette, and N. Ayache, "Automatic detection and segmentation of evolving processes in 3D medical images: Application to multiple sclerosis," *Medical Image Analysis,* vol. 6, pp. 163-179, 2002.

23- M. Rubeaux, N. Joshi, M. R. Dweck, A. Fletcher, M. Motwani, L. E. Thomson*, et al.*, "Demons versus Level-Set motion registration for coronary (18) F-sodium fluoride PET," *Proceedings of SPIE--the International Society for Optical Engineering,* vol. 9784, p. 97843Y, 03/21 2016.

24- G. Germano, P. B. Kavanagh, J. Chen, P. Waechter, H.-T. Su, H. Kiat*, et al.*, "Operator-less processing of myocardial perfusion SPECT studies," *Journal of Nuclear Medicine,* vol. 36, pp. 2127-2132, 1995.

25- P. J. Slomka, M. Rubeaux, L. Le Meunier, D. Dey, J. L. Lazewatsky, T. Pan*, et al.*, "Dual-gated motion-

frozen cardiac PET with flurpiridaz F 18," *Journal of Nuclear Medicine,* vol. 56, pp. 1876-1881, 2015.

26- M. Dawood, F. Gigengack, X. Jiang, and K. P. Schafers, "A mass conservation-based optical flow method for cardiac motion correction in 3D-PET," *Med Phys,* vol. 40, p. 012505, Jan 2013.

27- Y. Petibon, J. Ouyang, X. Zhu, C. Huang, T. G. Reese, S. Y. Chun, *et al.*, "Cardiac motion compensation and resolution modeling in simultaneous PET-MR: a cardiac lesion detection study," *Phys Med Biol,* vol. 58, pp. 2085-102, Apr 7 2013.

28- G. Germano, P. B. Kavanagh, P. Waechter, J. Areeda, S. Van Kriekinge, T. Sharir, *et al.*, "A new algorithm for the quantitation of myocardial perfusion SPECT. I: technical principles and reproducibility," *J Nucl Med,* vol. 41, pp. 712-9, Apr 2000.

29- L. Zhe, D. Deng, and W. Guang-Zhi, "Accuracy validation for medical image registration algorithms: a review," *Chin Med Sci J,* vol. 27, pp. 176-81, Sep 2012.

30- M. Dawood, C. Brune, X. Jiang, F. Büther, M. Burger, O. Schober, *et al.*, "A Continuity Equation Based Optical Flow Method for Cardiac Motion Correction in 3D PET Data," in *Medical Imaging and Augmented Reality: 5th International Workshop, MIAR 2010, Beijing, China, September 19-20, 2010. Proceedings*, H. Liao, P. J. E. Edwards, X. Pan, Y. Fan, and G.-Z. Yang, Eds., ed Berlin, Heidelberg: Springer Berlin Heidelberg, pp. 88-97, 2010.